

RSC Advances



This is an *Accepted Manuscript*, which has been through the Royal Society of Chemistry peer review process and has been accepted for publication.

Accepted Manuscripts are published online shortly after acceptance, before technical editing, formatting and proof reading. Using this free service, authors can make their results available to the community, in citable form, before we publish the edited article. This *Accepted Manuscript* will be replaced by the edited, formatted and paginated article as soon as this is available.

You can find more information about *Accepted Manuscripts* in the [Information for Authors](#).

Please note that technical editing may introduce minor changes to the text and/or graphics, which may alter content. The journal's standard [Terms & Conditions](#) and the [Ethical guidelines](#) still apply. In no event shall the Royal Society of Chemistry be held responsible for any errors or omissions in this *Accepted Manuscript* or any consequences arising from the use of any information it contains.

Cite this: DOI: 10.1039/c0xx00000x

www.rsc.org/xxxxxx

ARTICLE TYPE

Fabrication of Gold Nanoparticles on Biotin -di-Tryptophan Scaffold for Plausible Biomedical Applications[†]

Narendra Kumar Mishra,^a Vikas Kumar,^b Khashti Ballabh Joshi*^b

Received (in XXX, XXX) Xth XXXXXXXXX 20XX, Accepted Xth XXXXXXXXX
DOI: 10.1039/b000000

This study probes the beneficial role of biotinylated di-tryptophan for the synthesis and stabilization of gold nanoparticles (AuNPs) and concurrently these AuNPs were scattered inside the biotinylated spherical scaffold in a controlled manner. Such AuNPs peptide devices showed the effect of plasmonic heating and can be used for the plausible biomedical applications as theranostic agents.

Gold metallic nanoparticles are commonly used in the lab as a tracer, to detect the presence of specific proteins or DNA in a sample for example colloidal AuNPs labelled with biomolecules have wide range of applications in bioengineering, biomolecular imaging and molecular diagnostics.¹⁻⁸ For the passive and active targeted drug delivery, recently gold, magnetic and composite nanoparticles have been exploited.⁹⁻¹¹ The surface chemistry of gold nanoparticles, has been proven to be chemically versatile for loading biomolecules and optimizing physicochemical parameters.¹¹ In this context recently Gold nanorods (AuNRs) have also become attractive for biological applications due to their optoelectronic properties.¹³ Gold is used for nanoparticle applications because it is unreactive and isn't sensitive to air or light but gold does like to form bonds with itself. Therefore to avoid the aggregation of AuNPs their surface has to be covered with a layer of protective molecules.¹⁴ Sulphur is one of the few elements with which gold happily binds, so sulphur-containing groups are often used for this protective coating. These sulphur groups can also be functionalized by giving extra bits such as binding sites or fluorescent markers and can be picked up by a microscope.¹⁶⁻¹⁷

Besides sulphur, naturally binding agents nucleic acids, proteins, peptides and amino acids also used for the reduction or protective coating of gold.¹⁸⁻²² Glutamic acid¹⁹, Tyrosine²⁰ and tryptophan²² are well known reducing agent for gold and study also reveals that AuNPs quench tryptophan fluorescence several folds lower when added to tryptophan containing protein such as BSA.²⁰ The conjugation of AuNPs with biomolecules changes the optoelectronic properties of the particles, however, in most cases,²³ biomolecules also undergo some structural changes at the boundary surface of nanoparticles.²⁴⁻²⁶ Such kind of behaviour is of great importance in various biomedical applications, particularly drug delivery or receptor targeting.²⁷⁻²⁹

Tryptophan is an interesting aromatic amino acid in biochemistry for various applications due to the presence of indole ring in its side chain and have crucial photophysical and photochemical role in self assembly.³⁰ Tryptophan has been used as "reporter group" owing to its intrinsic fluorescence nature which is a very useful photophysical property in order to get the

3D information about the folded structures of biomolecules.³¹ It has also been found that unlike phenylalanine, di-tryptophan is unable to form ordered structures in solution.³² Therefore to get the ordered structures of tryptophan based short peptides, suitable chemical modifications are needed to increase the non-covalent interactions by employing desired chemical entities.³³⁻³⁶ In this context our previous report had proven that synthetic biotinylated peptide³⁷ **1** (Fig. 1), where biotin comprises with di-tryptophan peptide afforded rapid self-assembly in solution, leading to the formation of variable size of robust, superior and ordered nanostructures and markedly, these structures are responsive towards external stimuli, such as presence of small and large biomolecules and biologically active cations.³³⁻³⁶ Therefore the compound **1** is of particular interest and can be used for nanofabrication and also have exciting potential application for nanotechnology to create various class of biomaterial.³⁷

In the context of above findings and inspired from our previous work³⁷⁻³⁹ we synthesized the AuNPs with the help of **1** which worked as capping agents⁴⁰⁻⁴¹ for AuNPs and concurrently they were encapsulated by the spherical structures. Synthesis and biofabrication of AuNPs with peptides is of great interest owing to their biocompatibility and ease of functionality.⁴²⁻⁴⁵ The

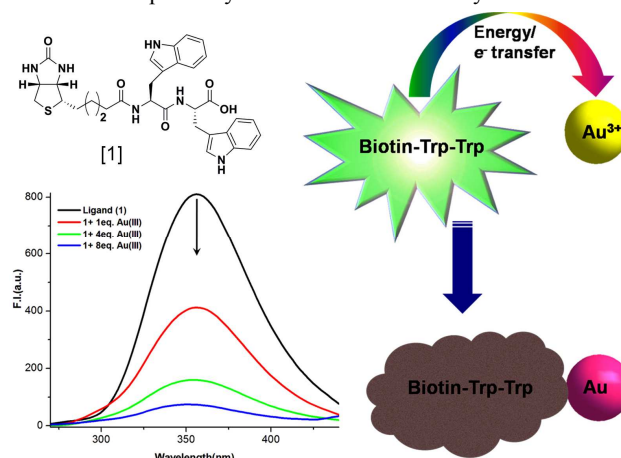


Figure 1. Fluorescence quenching of Biotin-Trp-Trp, **1** (10^{-5} M) by HAuCl₄ solution in methanol/water (1:1). Fluorescence intensity measured at $E_{em} = 358$ nm, after excitation at $E_{ex} = 280$ nm and corresponding possible mechanism of fluorescence quenching of **1** by AuNPs.

tumor-specific docking moieties such as peptide conjugated nanoparticles predominantly interact with their corresponding biomolecules which are overexpressed in tumors such as conjugation of AuNPs to folic acid⁴⁶, anti-EGFR antibody⁴⁷ and

tumor necrosis factor (TNF).⁴⁷ Therefore AuNPs-Peptide hybrids can act as theranostic agent which can show minimal systemic side effects in real-time clinical applications.⁴⁸⁻⁴⁹

In this paper we report the facile synthesis and fabrication of gold nanoparticles with the help of **1**, where AuNPs encapsulated by the soft structure of **1**. The Biotin conjugated peptide containing tryptophan group quenches its fluorescence via the energy transfer mechanism (Fig. 1) in the presence of gold nanoparticles. Therefore, the ability to synthesize nanoparticles of controlled size and shape with the help of small peptides or biomolecules is highly desirable and the effects of these AuNPs on the molecular and supramolecular ensembles were investigated by various spectroscopic, spectrometric and microscopic techniques.

Based on our interest in peptide self-assembly and nanotechnology,³³⁻³⁸ we decided to explore interaction of **1**, comprising of tryptophan and biotin, with Gold metallic ions by recording the fluorescence intensity at its emission wavelength 358 nm. We have observed that the addition of Au(III) ions to the solution of **1** resulted the significant changes (Fig. 1) in fluorescence intensity which is well corresponded for tryptophan containing peptides and protein.³⁸ The observed quenching may be attributed to an electrostatic interaction of Au(III) ions with Trp indole moiety leading to energy transfer from Trp residue to Au(III).

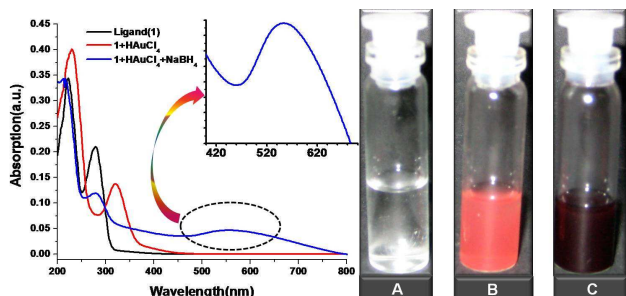


Figure 2. Left:-UV/Vis spectra of **1** (black line), **1** in the presence of Au(III) solution (red Line) and after reduction with NaBH₄ (blue line). Inset:- SPR band. Right:- Visual detection of color change of **1** (50% aq. methanol) in the presence of Au(III) ions and upon reduction with NaBH₄, A)-10 mM solution of **1** in 50% methanol/water, B)- after addition of HAuCl₄ and C)- followed by NaBH₄ reduction.

Colorless solution of **1** turned into yellowish orange upon addition of HAuCl₄ solution, which clearly reveals that the complex formation occurs between the molecules of **1** and Au(III) ions. The yellowish orange color converted to deep ruby red when reduced with sodium borohydride (Fig. 2). The color change is in accordance with literature reports and also the plasmonic characteristic of gold nanoparticles. Compound **1** displayed typical absorption peaks at 224 and ~280 nm in the UV-Vis spectrum (Fig. 2), which are due to the presence of amide and tryptophan, group respectively. It is interesting to note that both the absorption bands are red shifted and this red shift upon addition of Au(III) solution to neat solution of peptide also indicates that the peptide **1** making strong complex with Au(III) ions.³⁸

Since compound **1** is well known for assembling rapidly into vesicles in solution state³⁷, therefore we wish to check the fate of these vesicles after interaction with Au(III) ions. The study carried out with the incubation of 1 eq. of metal ion salts to 1 mM solution of **1** and imaged under transmission electron microscope (TEM) to know the exact condition of Au(III) ions treated

vesicles. We found that nanoparticles are encapsulated by vesicles of **1** (Fig. 3b, c). The vesicular morphologies of **1** are intact in the presence of Au(III) ions in solution. Therefore to know the nature of these nanoparticles we have taken the selected area electron diffraction (SAED) patterns which showed that encapsulated nanoparticles have crystalline unit cell structure (Fig. S4) which is further confirmed by the XRD (Fig. 3d). The XRD pattern of these nanoparticles are well corresponded with face centered cubic (fcc) unit cell of Au(III) ions which have (111), (200), (220), (311) strong Bragg reflections of fcc gold.⁵⁰

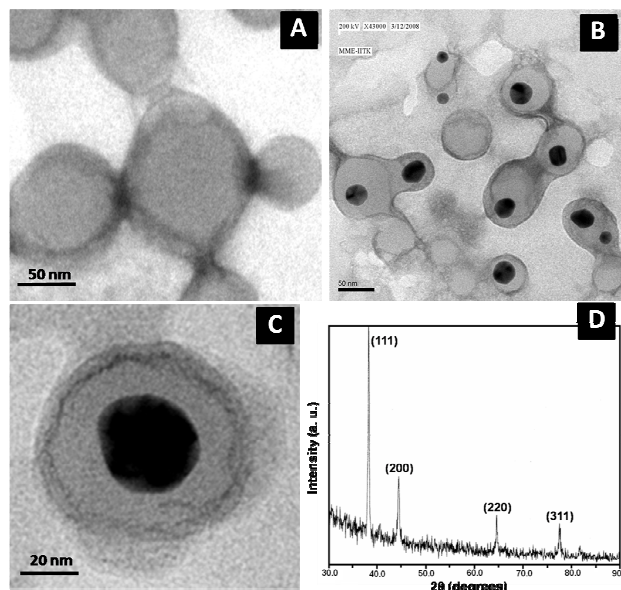


Figure 3: TEM micrograph of (A) intact vesicles of **1**, (B-C) Au(I)NPs bounded spherical structures and magnified vesicle and (D) XRD pattern of a AuCl₄-Peptide **1** coated film deposited on a glass substrate representing face centred cubic (fcc) gold unit cell structure.

The preliminary spectroscopic and microscopic investigation motivated us to check the structural changes in **1** after the addition of Au(III) ions by ¹H NMR measurements. The HPLC purified sample of **1** in DMSO-*d*₆ (Fig. 4 bottom blue trace) was titrated with increasing amount of aqueous solution of HAuCl₄ in order to understand the effect of Au(III) ions in **1** during the complex formation process. The spectra depict that Trp-indole-NH, Trp-arH and amide-NH protons showed a remarkable up field shift upon incremental addition of HAuCl₄ solution. However we observed that the ureido-NH protons of biotin group were disappeared (Fig. 4 blue to red trace; marked by red arrow). This study suggests that the loss of two hydrogens from the biotin's ureido group are responsible for the complexation and perhaps during this process the reduction of Au(III) to Au(I) ions take place. This observation can be supported by the observation of red shift in UV-Vis followed by changes in the color (Fig. 2). Further the complex formation is stabilized by the Trp-indole moiety of **1** and perhaps acts as a capping agent to stabilize the nanoparticles in the solution. Such kind of strong interaction affects the electronic environment of the key protons of **1**, hence shifting them up-field.

Next to determine the conformational changes in **1** in the presence and absence of Au(III) solutions, we have done the circular dichroism (CD) study.⁵¹ Owing to the indole side chain, tryptophan has a specific CD spectrum which depends strongly

upon the conformation of peptide and ambient polarity. The conjugation of D-Biotin and Trp-Trp residue resulted **1** thus it contains two naturally occurring fragments vitamin D-Biotin and Trp-Trp dipeptide respectively. After studying the self-assembling behaviour of D-biotin, biotin methyl ester³⁷ and **1**, we were interested to check the secondary structure of these components with the help of circular dichroism (CD) study (Fig. 5). The 1 mM solution of **1** in 50% aqueous methanol was

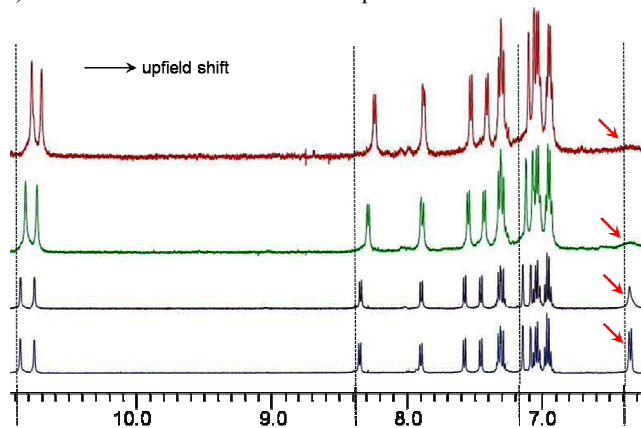


Figure 4. ¹H NMR titration spectra of **1** in DMSO-*d*₆ in the presence of increasing amount of AuCl₄ solution.

recorded and found that the **1** has random coil like secondary structure. It is obvious that the positive extremum band at 233 nm and negative extremum band at 210 nm owing to the presence of biotin group and the Trp-Trp group respectively.⁵²⁻⁵³ However the CD spectra of Trp-Trp in water shows a negative extremum at 201 nm and positive extremum at 220 nm.⁵³ Hence it was predicted that the CD spectra of **1** in methanol/water will also

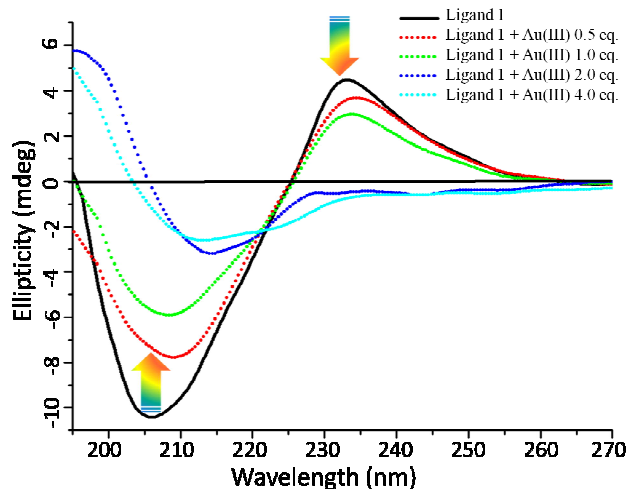


Figure 5: CD titration of Au(III) ion solution (in water) with **1** (0.5 mM in 50% aqueous methanol).

have combined effect of biotin and trp chromophore and responsible for the band centered at 233 nm and 210 nm. Therefore compound **1** shows a characteristic CD signal with negative extremum at 225 nm and positive extremum centered at ~210 nm in the far UV-region.⁵⁴ Changes in the ellipticity values are useful probes for visualizing variation in conformational

change and hence self assembly. These observation confirmed

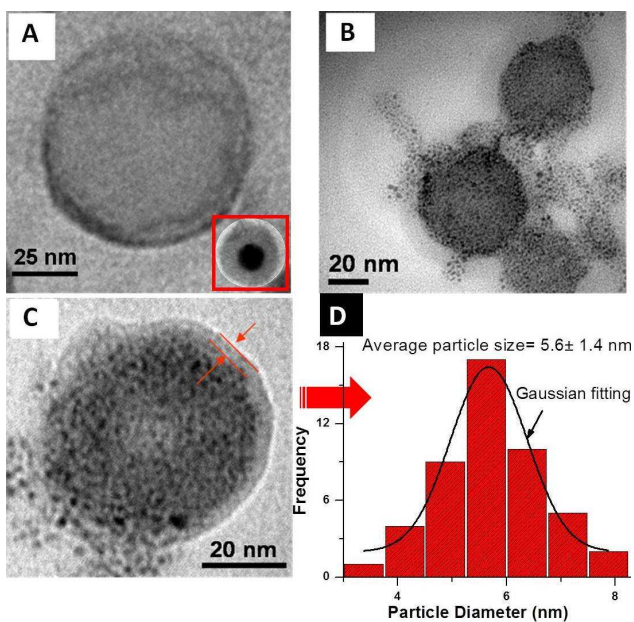


Figure 6: (A) TEM micrograph of **1** before addition of HAuCl₄ solution (inset : after addition of HAuCl₄ solution) (B, C) images of smaller size self organized AuNPs on the surfaces of Biotin -di-Trptophan scaffold after NaBH₄ reduction (D) corresponding particle size distribution histogram of AuNPs.

that **1** undergoes a more flexible conformational state on the boundary surface of nanoparticles (Fig. 5).^{20, 53}

The decomposition of big size of nanopartilces can be easily achieved through redox reaction in the presence of NaBH₄ (0.1 M at 25 °C).⁵⁴ Reduction of the bigger nanopartilces gave products mainly containing a large quantity of fused AuNPs which were encapsulated by capsules of **1** during complexation stage now were decomposed and defused inside without causing any defect in the morphology (Fig. 6A, B and C). Per vesicle AuNPs particle size distribution histogram and subsequently Gaussian fitting, reveals that the average diameter of the NaBH₄ treated nanoparticles are 5 -7 nm (Fig. 6D). The appearance of an SPR band (530 nm) of the Au nanoparticles further confirmed the size of AuNPs owing to the reduction reaction of NaBH₄ (Fig 2).

It was still not clear whether these AuNPs are inside⁵⁵ the surface or deposited over the surface of the spherical morphology of **1**. Therefore we wished to take the atomic force microscopic images of **1** before and after the reduction of NaBH₄. The AFM images of the fresh sample of **1** in the absence of AuNPs displayed clear images of vesicles (Fig.7A and B) which do not show any kind of encapsulation inside the soft structures (Fig 7b, 3D image). However in the presence of AuNPs, encapsulation of the partilces were clearly visible which can be further confirm by 2D and 3D images of the multiple and single vesicles (Fig 7C, D and E) and these observations are well corresponded with TEM images of figure 7F and figure 6C (marked by red arrow). Observations from the 3D images of AFM reveals that there is no deposition found along and outside edge of the vesicles therefore all the AuNPs are encapsulated. Moreover, the TEM observations reveal that the excess addition of HAuCl₄ solution into **1** followed by reduction with NaBH₄ does not affect the morphology of **1**. However more numbers of defused AuNPs with smaller size get encapsulated and deposited over the surface (Fig. 7F).⁵⁶⁻⁵⁷

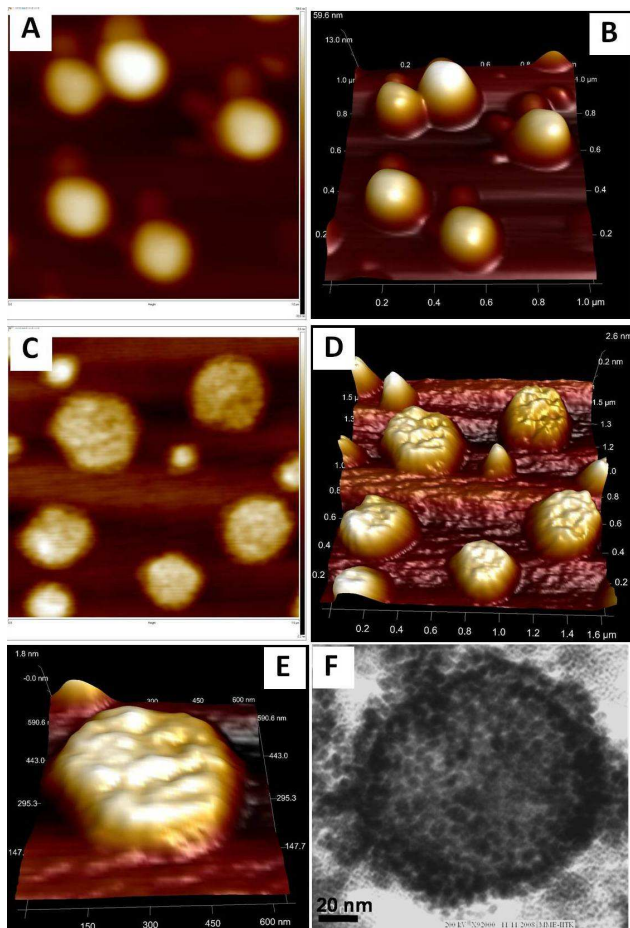


Figure 7: (A, B) 2D and 3D AFM micrographs of intact vesicles of **1** (C, D), 2D and 3D images showing encapsulations of AuNPs with **1**, (E) real time magnified AFM image of AuNPs loaded vesicle and (F) corresponding TEM image of AuNPs loaded vesicle.

This observation was supported by the UV-Vis experiments where the red shift was observed upon the addition of HAuCl_4 solution which is retained back in its original shape along with the development of SPR band when treated with NaBH_4 solution. The identity of these nanoparticles was also confirmed with an EDAX analyzer that was embedded to TEM where the spectral pattern of these particles showed that the particles are made up of the Au with large carbon content (Fig.S5) which perhaps from organic source, **1** and carbon coated substrate.

Encapsulated gold nanoparticles are very important among the other most common nanoparticles which are studied for biomedical applications.^{3,9} The specific applications of AuNPs-hybrids are to diagnose and treat the various ailments and therefore have placed them in the category of theranostic agents. As AuNPs cannot directly interact with the living tissues therefore to facilitate the biological interactions the AuNPs encapsulated peptide devices can be used as a carrier which could reduce time and cost transitioning from diagnostic to treatment.

There is still a much attention is required to use such devices as theranostic agents. Owing to the unique optoelectronic properties of AuNPs they can absorb light intensely and convert it to the non-invasive heat inside the targeted tissue area for biomedical applications. Therefore we have also tried to show the effect of the plasmonic heating on these AuNPs encapsulated peptide devices and found very interesting results (Fig. 8). We have taken Rhodamine B solution and incubated with the solution of self assembled structures of AuNPs fabricated scaffold of **1**.

As dye interacted with AuNPs-**1** hybrid structures bright red colored spherical objects were appeared under dark field fluorescence microscope (Fig: 8A). When this rhodamine loaded vesicles exposed to sunlight for 30 minutes, owing to prolonged plasmonic heating the dye encapsulated by the AuNPs-**1** hybrid structures released out which appear at the periphery of the deformed vesicles (Fig: 8B), which can be very useful for controlled drug release.^{36,38} Further to confirm these observations

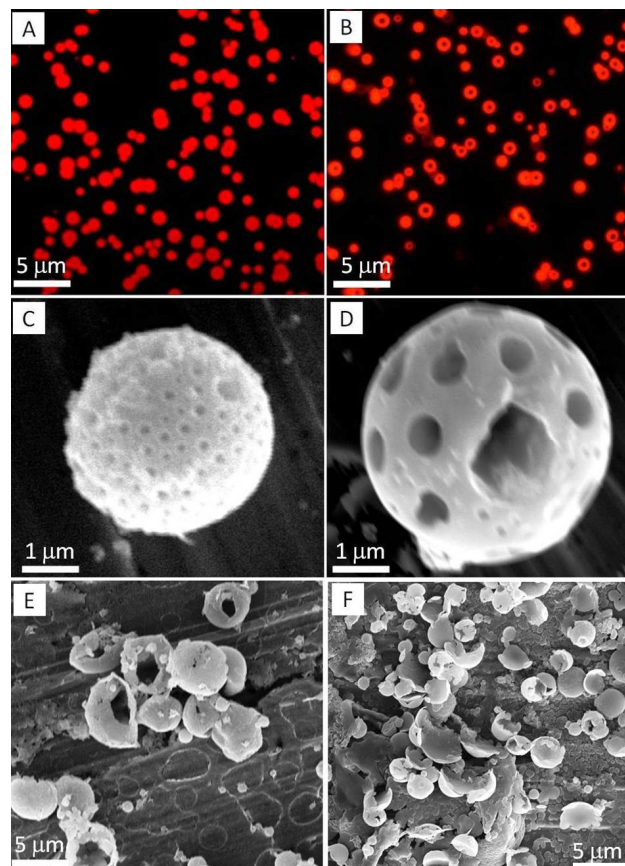


Figure 8: *Top:* OM micrograph of (A) AuNPs encapsulated vesicles incubated with Rhodamine B dye shows that it is encapsulating by these hybrid spherical structures, (B) upon 30 minutes exposure of the sunlight, dye is released from the vesicles due to the plasmonic heating. *Bottom:* SEM micrographs depicts time dependent effect of plasmonic heating on the AuNPs loaded vesicles of **1**; (C) at time 5 minutes the vesicle started melting which can be seen by the appearance of small pores and (D) they get converted into large size after 10 minutes of sunlight exposure. (E), after 15 minutes few of these AuNPs loaded vesicles get deformed and disrupted which upon prolonged (25-30 minutes, Fig 8F) exposure of sunlight entirely disrupted

we have performed the time dependent effect of plasmonic heating on such devices and found very interesting results. We kept the solution of AuNPs loaded vesicles under sunlight and prepared the sample for SEM at different time intervals followed by imaging under scanning electron microscope. The time dependent SEM observations reveal that AuNPs loaded vesicles are changing their shape via appearance of bigger pores on the surface of vesicle which get converted into bigger sizes after 10 minutes of exposure (Fig. 8C and D) of sunlight. After 15 min exposure of sunlight these AuNPs loaded vesicles started altering the shape and finally upon longer exposure up to 30 minutes get entirely disrupted (Fig. 8F).

At this stage, to get more insight into these plasmonic heating based disruption of AuNPs loaded vesicles, we have investigated these findings with the help of liquid cell AFM imaging too. We kept the solution of **1** without HAuCl₄ into sunlight for 30

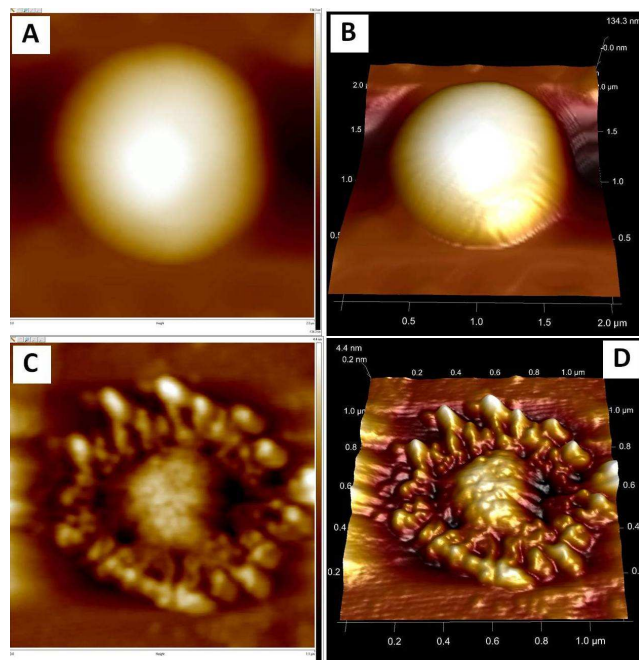


Figure 9: (A) Liquid cell imaging of solution **1** which was kept under sunlight for 30 minutes and (B) corresponding 3D image. (C) Liquid cell imaging of AuNPs loaded solution of **1** after long exposure of sunlight and (D) corresponding 3D image. These images reveals that the effect of plasmonic heating and the potential application for theranostic application.

minutes and took the images of single vesicle of **1** without the addition of HAuCl₄ solution and subsequently images of AuNPs loaded vesicles after the prolonged exposure of sunlight. Interestingly we observed a very clear and well shaped AFM image of intact vesicle (Fig. 9A and B) of solution **1** and disrupted vesicle of AuNPs incubated sample (Fig 9C and D). These observations demonstrated that the effect of sunlight upon the AuNPs loaded vesicles is due to the plasmonic heating and not by just solvent evaporations.

A schematic proposed model depicts the formation of spherical structures in solution state^{38,55} which upon addition of HAuCl₄ solution retained (Fig. 10). However based on our experimental observation the Au(III) ions were interacted to **1** and formed a complex followed by encapsulation by these spherical scaffold. Upon reduction with NaBH₄, break down of bigger nanoparticles to smaller one and diffused inside the vesicles of **1** (Fig. 6 and 7). It could be proposed that the binding of **1** with Au(III) affords a rapid approach toward the synthesis of AuNPs, which is suitably dispersed after the treatment of NaBH₄ solution and these peptide based soft structures worked as a scaffold for AuNPs.

In conclusion, we have developed the utility of small peptide conjugate by simple one-pot synthesis of stable gold nanoparticles by using simple solution phase treatment. The AuNPs were homogeneously decorated inside the the biotin -di-tryptophan scaffold and investigated by various spectroscopic and microscopic techniques. Our results highlight that the biotinylated peptide-gold nanoparticles (AuNPs) can be scattered on the

scaffold and loading of AuNPs can be controlled. The small peptide stabilizes nanoparticles and could potentially serve as a

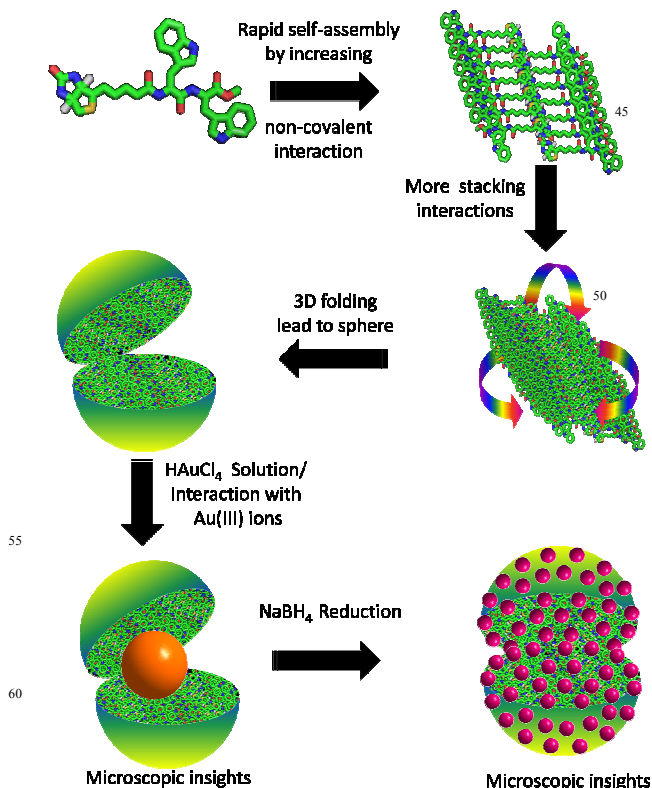


Figure 10. Proposed model for AuNPs formation followed by encapsulation by Biotin-di-Tryptophan Scaffold.

viable alternative to chemical methods. Design of such peptide can be used to develop multifunctional peptides that can be useful in biosensing applications, targeting gold nanoparticles into cells etc. Further these AuNPs encapsulated peptide devices can be used as diagnostic agents and treatments of various ailments, hence can work as theranostic agents.

NKM and VK thank CSIR- India and NFOBC-UGC- India for pre-doctoral research fellowship respectively. Special thanks to Prof. Sandeep Verma IIT-Kapur India for his constant support and invaluable discussions during the work and providing the research facility. Authors thank to SIC- Dr. H.S.G. central university Sagar-India for providing AFM and SEM facility. This work is supported by UGC-BSR scheme to KBJ from university Grant Commission (UGC), India.

Notes and references

- ⁸⁵ ^bDr. Harisingh Gour Central University Sagar (MP), 470003, India. E-mail(s): kbjoshi@dhsu.ac.in and kbjoshi77@gmail.com
⁸⁶ ^aDepartment of Chemistry Indian Institute of Technology Kanpur, Kanpur-208016,
⁸⁷ [†] Electronic Supplementary Information (ESI) available: See DOI: 10.1039/b000000x/
⁸⁸ [‡] **General-** Methanol, Water, HAuCl₄, NaBH₄ were purchased from Spectrochem, Mumbai, India, and used without further purification.
⁸⁹ **Atomic Force Microscopy (AFM)** – Neat and co-incubated solution of Biotin–Trp–Trp peptide sample (**1**) with gold was imaged with an atomic force microscope. The Samples were placed on freshly cleaved HOPG and muscovite mica surfaces followed by imaging with an atomic force

microscope (INNOVA, ICON Analytical Equipment, Bruker, Sophisticated Instrument Center-Dr. Hari Singh Gour Central University, Sagar-M.P.) operating under the Acoustic AC mode (AAC or Tapping mode), with the aid of a cantilever (NSC 12(c) from MikroMasch, Silicon Nitride Tip) by NanoDrive™ version 8 software. The force constant was 2.0 N/m, while the resonant frequency was 284.60 kHz. The images were taken in air at room temperature, with the scan speed of 1.5-2.0 lines/sec. The data analysis was done using of Nanoscope Analysis Software. The sample-coated substrates were dried at dust free space under 60W lamp for 6h followed by high vacuum drying and subsequently examined under AFM. **Scanning Electron Microscopy (SEM):** A highly oriented pyrolytic graphite surface (HOPG) was used as substrate. 10 μ L aliquotes of each samples were placed on it and the samples were air dried and were directly mounted on the stage under native conditions and an image was taken for each sample with the help of high resolution scanning electron microscope dual beam system (NOVA 600 NANOLAB, D97 FEI) operating at WD 10.6 mm and 20 kV. **Transmission Electron Microscopy (TEM)** – The samples were placed on a 400 mesh carbon coated copper grid. After 1 minute, excess fluid was removed and the grid was/wasn't negatively stained with 2% uranyl acetate solution. Excess stain was removed from the grid and the samples were viewed using a FEI Technai 20 U Twin Transmission Electron Microscope operating at 80 kV. The microscope is a STEM and is also equipped with a EDS detector, HAADF detector and Gatan digital imaging system. **Energy Dispersive X-ray analysis (EDAX) by TEM embedded analyzer-** The TEM has an EDAX facility which contains the EDAX unit with a detector Super Ultra Thin Window (Super UTW) used for capturing of x-rays, and the spectroscopic analysis was done by the EDAX GenesisVersion 3.60 software system. **X-Ray diffraction measurements-** X-Ray diffraction (XRD) analysis of drop-coated films on glass substrates of the Au(I)NPs capped vesicles of sample 1 was carried out on a ARLX'TRA, X-ray Diffractometer (Thermo electron corporation) instrument operating at 40 kV and a current of 30 mA with $\text{Cu-K}\alpha$ ($\lambda = 1.451841\text{\AA}$) radiation. **Fluorescence studies-** Fluorescence spectra were recorded on Varian Luminescence Cary eclipsed and CARY win 100 Bio UV-Vis spectrophotometer with a 10 mm quartz cell at 25 ± 0.1 °C. The solutions of 1 and metal salts were prepared in $\text{CH}_3\text{OH}/\text{H}_2\text{O}$ (50:50). Deionized water and methanol (HPLC grade) were used in these studies. The solutions containing 1 (10^{-5} M) and different concentrations of metal salt were prepared in $\text{CH}_3\text{OH}/\text{H}_2\text{O}$ (50:50) and were kept at 25 ± 1 °C for 0-24 h and recorded their fluorescence spectra at fresh as well as aged conditions. All fluorescence scans were saved as ACSII files and further processed in Excel™ to produce all graphs shown. **Preparation of AuNPs:** The HAuCl_4 -1 hybrid colloid samples were prepared according to the following procedure: First, 1 mL of 50% aqueous methanol solution of 1 (1mM) was added into 1 mL of water in a 10 mL round bottom flask. Aqueous solution of HAuCl_4 (1 mL, 4 mM) was then introduced into the resulting solution under rigorous stirring at room temperature. A gradual color change from colorless to yellowish orange was observed and a large amount of precipitate occurred after 1hr. When the stirring was stopped. The solution was further stirred for 2 h. The colloid samples thus prepared were used directly for characterization without further treatment. The as-prepared colloidal particles can be easily decomposed through redox reaction of HAuCl_4 contained therein with NaBH_4 . The reduction of the colloidal particles gave products mainly containing a large quantity of fused gold nanoparticles with mean diameter 6-7 nm, indicating that the larger networking present at the complete prereluction stage was decomposed after reduction with NaBH_4 . The XRD and UV-Vis studies further confirm the formation of nanoparticles. **Purification of gold nanoparticle colloid:** Purification of gold nanoparticle colloid done by using centrifugation method before using it for the imaging/analysis. After the formation of AuNPs-Peptide hybrids the solution was centrifuged at 12,000g for 20-30 minutes followed by removal of the supernatant and washing with methanol. The residue/pallets were re-dissolved in the 50% aqueous methanol in the appropriate volume of solvent. The colloid solution was stable for several days.

1. M.C. Daniel & D. Astruc, *Chem. Rev.*, 2004, **104**, 293-346.

2. X. Huang, S. Neretina and M. A. El-Sayed, *Adv. Mater.*, 2009, **21**, 4880-4910.

3. E. Katz and I. Willner *Angew. Chem. Int. Ed.* 2004, **43**, 6042-6408.

4. A. Wijaya, S. B. Schaffer, I. G. Pallares and K. Hamad-Schifferli, *ACS Nano*, 2009, **3**, 80–86,

5. C. F. Shaw, *Chem Rev.*, 1999, **99**, 2589-2600.

6. M. De, P. S. Ghosh and V. M. Rotello *Adv. Mater.*, 2008, **20**, 4225-4241.

7. I. H. El-Sayed, X. Huang and M. A. El-Sayed, *Nano Lett.*, 2005, **5**, 829-834.

8. C. J. Murphy, A. M. Gole, J. W. Stone, P. N. Sisco, A. M. Alkilany, E. C. Goldsmith and S. C. Baxter, *Acc. Chem. Res.*, 2008, **41**, 1721-1730.

9. D. A. Giljohann, D. S. Seferos W. L. Daniel and M. D. Massich P. C. Patel and C. A. Mirkin *Angew. Chem. Int. Ed.*, 2010, **49**, 3280-3294.

10. S. Son, J. Nam, J. Kim, S. Kim and W. J. Kim, *ACS Nano*, 2014, **8**, 5574-5584.

11. J. Kim, Y. M. Lee, Y. Kang, and W. J. Kim, *ACS Nano*, 2014, **8**, 9358-9367.

12. J. Yu, X. Chu and Y. Hou, *Chem Commun.*, 2014, **50**, 11614-11630.

13. X. Huang, I. H. Ei.- Sayed, W. Qian and M. A. Ei-Sayed, *J. Am. Chem. Soc.*, 2006, **128**, 2115-2120.

14. R. Levy, N. T. K. Thanh, R. C. Doty, I. Hussain, R. J. Nichols, D. J. Schiffrin, M. Brust and D.G. Fernig, *J. Am. Chem. Soc* 2004, **126**, 10076-10084.

15. Z. Zhang, J. Wang, X. Nie, T. Wen, Y. Ji, X. Wu, Y. Zhao and C. Chen, *J. Am. Chem. Soc.*, 2014, **136**, 7317-7326.

16. E. Pensa, E. Cortes, G. Corthey, P. Carro, C. Vericat, M. H. Fonticelli, G. Benitez, A. A. Rubert and R. C. Salvarezza, *Acc. Chem. Res.*, 2012, **45**, 1183-1192.

17. P. Joshi, V. Shewale and R. Pandey, *J. Phys. Chem. C.*, 2011, **115**, 22818-22826.

18. Y. Ding, Z. Jiang, K. Saha, C. S. Kim, S. T. Kim, R. F. Landis and V. M. Rotello *Mol. Ther.* 2014 DOI:10.1038/mt.2014.30.

19. T. Serizawa, Yu. Hirai and M. Aizawa, *Langmuir*, 2009, **25**, 12229–12234.

20. N. Wangoo, K. K. Bhasin, S. K. Mehta and C. R. Suri, *J. Coll. Int. Sci.* 2008, **323**, 247-254.

21. R. R. Selvakannan, A. Swami, D. Srithiyarayanan, P. S. Shirude, R. Pasricha, A. B. Mandale and M. Sastry, *Langmuir*, 2004, **20**, 7825-7836.

22. P. R. Selvakannan, S. Mandal, S. Phadtare, A. Gole, R. Pasricha, S.D. Adyanthaya and M. Sastri, *J. Colloid. Interface Sci.*, 2004, **269**, 97-102.

23. A. K. Nowinski, A. D. White, A. J. Keefe and S. Jiang, *Langmuir*, 2014, **30**, 1864-1870.

24. S. H. Brewer, W. R. Glomm, M. C. Johnson, M. K. Knag and S. Franzen, *Langmuir*, 2005, **21**, 9303-9307.

25. B. Dubertret, M. Calame, and A. J. Libchaber, *Nature Biotechnology*, 2001, **19**, 365-370.

26. M. Mahmoudi, I. Lynch, M. R. Ejteahadi, M. P. Monopoli, F. B. Bombelli and S. Laurent, *Chem. Rev.*, 2011, **111**, 5610-5637.

27. A. Verma, and V. M. Rotello, *Chem. Commun.*, 2005, 303–312.

28. R. Prades, S. Guerrero, E. Araya, C. Molina, E. Salas, E. Zurita, J. Selva, G. Egea, C. L. Iglesias, M. Teixido, M. J. Kogan and E. Giralt, *Biomaterials* 2012, **33**, 7194-7205.

29. H. Jans and Q. Huo, *Chem Soc Rev.*, 2012, **41**, 2849-2866.

30. E. Abel, S. L. D. Wall, W. B. Edward, S. Lalitha, D. F. Covey and G. W. Gokel, *Chem. Commun.*, 2000, 433-434.

31. Y. Chen and M. D. Berkley, *Biochemistry* 1998, **37**, 9976-9982.

32. M. Reches, and E. Gazit, *Science* 2003, **300**, 625-627.

33. S. Ghosh, M. Reches, Gazit E and S. Verma. *Angew. Chem., Int. Ed.* 2007, **46**, 2002-2004.

34. S. Ghosh., S. K. Singh and S. Verma *Chem. Commun.*, 2007, 2296-2298.

35. S. Ghosh, P. Singh and S. Verma, *Tetrahedron*, 2008, **64**, 1250-1256

36. A. K. Barman and S. Verma *Chem. Commun.* 2010; **46**: 6992-6994.

37. K. B. Joshi and S. Verma *Angew. Chem. Int. Ed.* 2008, **47**, 2860-2863.
38. N. K. Mishra, K. B. Joshi and S. Verma *J. Colloid. Inter. Sci.* 2015, **455**, 145-153.
- 5 39. K. B. Joshi, P. Singh and S. Verma, *Biofabrication* 2009, **1**, 025002.
40. S. Si, R. R. Bhattacharjee, A. Banerjee and T. K. Mandal, *Chem. Eur. J.*, 2006, **12**, 1256–1265.
- 10 41. S. Si, E. Dinda and T. K. Mandal, *Chem. Eur. J.* 2007, **13**, 9850-9861.
42. S. Si, and T. K. Mandal, *Chem. Eur. J.* 2007, **13**, 3160 – 3168.
43. J. M. Slocik, M. O. Stone and R. R. Naik, *Small*, 2005, **1**, 1048-1052,
- 15 44. C. L. Chen and N. L. Rosi, *Angew. Chem. Int. Ed.*, 2010, **49**, 1924-1942.
45. C. Zhang, C. Song, H. C. Fry and N. L. Rosi *Chem. Eur. J.* 2014, **6**, 6458-6462.
46. V. Dixit, J. V. D. Bossche, D. M. Sherman, D. H. Thompson and R. P. Andres, *Bioconjugate Chem.* 2006, **17**, 603-609.
- 20 47. K. Sokolov, M. Follen, J. Aaron, I. Pavlova, A. Malpica, R. Lotan and R. R. Kortum, *Canc. Res.* 2003, **63**, 1999-2004.
48. I. H. El-Sayed, X. Huang and M. A. El-Sayed, *Nano Lett.* 2005, **5**, 829-834.
- 25 49. M. P. Melancon, M. Zhou and C. Li., *Acc. Chem. Res.*, 2011, **44**, 947-956.
50. Y. Chen, X. Gu, C.-G. Nie, Z.-Y. Jiang, Z. X. Xie. and C. J. Lin *Chem. Commun.*, 2005, 4181–4183.
51. N. M. Green, W. P. Mose, P.M. Scopes *J. Chem. Soc. (C)*, 1970, 1330-1333
- 30 52. S. M. Kelly, N. C. Price *Curr. Pro. Pep. Sci.*, 2000, **1**, 349-384.
53. H. E. Auer, *J. Am. Chem. Soc.*, 1973, **95**, 3003-3011.
54. H. Wei, B. Li, Y. Du, S. Dong and E. Wang, *Chem. Mater.* 2007, **19**, 2987-2993
- 35 55. R. M. Gorgoll, T. Tsubota, K. Harano, and E. Nakamura, *J. Am. Chem. Soci.* 2015, DOI: 10.1021/jacs.5b03632.
56. T. Sawada, T. Takahashi, and H. Mihara, *J. Am. Chem. Soc.*, 2009, **131**, 14434-14441.
- 40 57. R. Contreras-Cáceres, J. Pacifico, I. Pastoriza-Santos, J. Pe´rez-Juste, A. Ferná´ndez, Barbero and L. M. Liz-Marza´n, *Adv. Funct. Mater.* 2009, **19**, 3070–3076.
- 45
- 50
- 55
- 60
- 65